SF2A 2013
L. Cambrésy, F. Martins, E. Nuss and A. Palacios (eds)

SATURN'S STRATOSPHERIC TEMPERATURE AND COMPOSITION FROM CASSINI/CIRS

S. Guerlet[1], T. Fouchet[2], B. Bézard[2], A. Spiga[1], M. Sylvestre[1,2], J. Moses[3] and F.M. Flasar[4]

Abstract. We present a short review of our current knowledge on Saturn's stratospheric thermal structure and composition (hydrocarbons) based on recent Cassini/CIRS observations. Anomalies in the temperature field and in the meridional distribution of hydrocarbons hint at atmospheric dynamical phenomena at play. The two most notable features are an obseved asymmetry in the hydrocarbons distribution at high altitudes, hinting at inter-hemispheric transport, and the discovery of an equatorial oscillation in temperature and zonal wind, hinting at interactions between vertically-propagating waves and the mean zonal flow. The physical processes behind these observed anomalies need to be better understood, and these results advocate for the development of climate models of Saturn's stratosphere.

Keywords: Saturn, Cassini

1 Introduction

Saturn's stratosphere is host to a rich hydrocarbon photochemistry initiated by the photolysis of methane (CH_4) near the homopause level that produces various hydrocarbons, from the main products ethane (C_2H_6) and acetylene (C_2H_2) to benzene (C_6H_6). Their meridional distribution and their variations with altitude and time (seasons) are governed by coupled photochemical and dynamical processes. Saturn's stratospheric circulation is still poorly known, as direct wind measurements are lacking. However, detailed measurements of hydrocarbons' meridional distribution and their vertical gradients can provide indirect constraints on atmospheric meridional and vertical transport. In addition, anomalies in the temperature field can also reveal atmospheric dynamical phenomenon at play.

Saturn's stratosphere can be probed by mid-infrared spectroscopic measurements. Onboard the Cassini spacecraft, the Composite and Infrared Spectrometer (CIRS) measures spectra of Saturn's thermal emission in the range 10–1400 cm^{-1}, with a spectral resolution tunable between 0.5 and 15.5 cm^{-1}. CIRS comprises three focal planes (FP1, FP3 and FP4), with FP3 and FP4 consisting of two linear arrays of ten detectors. Their individual projected field of view is typically 70km on Saturn, ie. 1 to 1.5 scale height. In limb viewing geometry, each detector probes a different altitude, allowing the retrieval of atmospheric profiles with a good vertical extent and resolution. We use a line-by-line radiative transfer model coupled to a constrained linear inverse method to first retrieve a temperature vertical profile from the analysis of the CH_4 emission band centered at 1305 cm^{-1} and from the H2-He collision-induced emission (590-660 cm^{-1}). Typically, using limb data, the temperature profile is constrained between 20 mbar and a few microbars, while nadir observations probe the stratospheric temperature in the range 5–0.5 mbar (see Fig. 1 for a typical temperature profile of Saturn's atmosphere along with the vertical sensitivity of Cassini/CIRS nadir and limb data). Once the temperature is constrained, we retrieve the volume mixing ratio vertical profiles of five hydrocarbons from their emission bands: C_2H_6 (centered at 822 cm^{-1}), C_2H_2 (730 cm^{-1}), C_3H_8 (748 cm^{-1}), C_4H_2 (628 cm^{-1}) and C_3H_4 (633 cm^{-1}).

Hereafter, we review results obtained from Cassini/CIRS data analysis (between 2005 and 2010, coresponding to mid-summer to autumn in the southern hemisphere) and their implications for Saturn's stratospheric dynamics.

[1] Laboratoire de Meteorologie Dynamique/IPSL/CNRS, Paris, France
[2] LESIA/Observatoire de Paris, Meudon, France
[3] Space Science Institute, TX, USA
[4] NASA/GSFC, Greenbelt, MD, USA

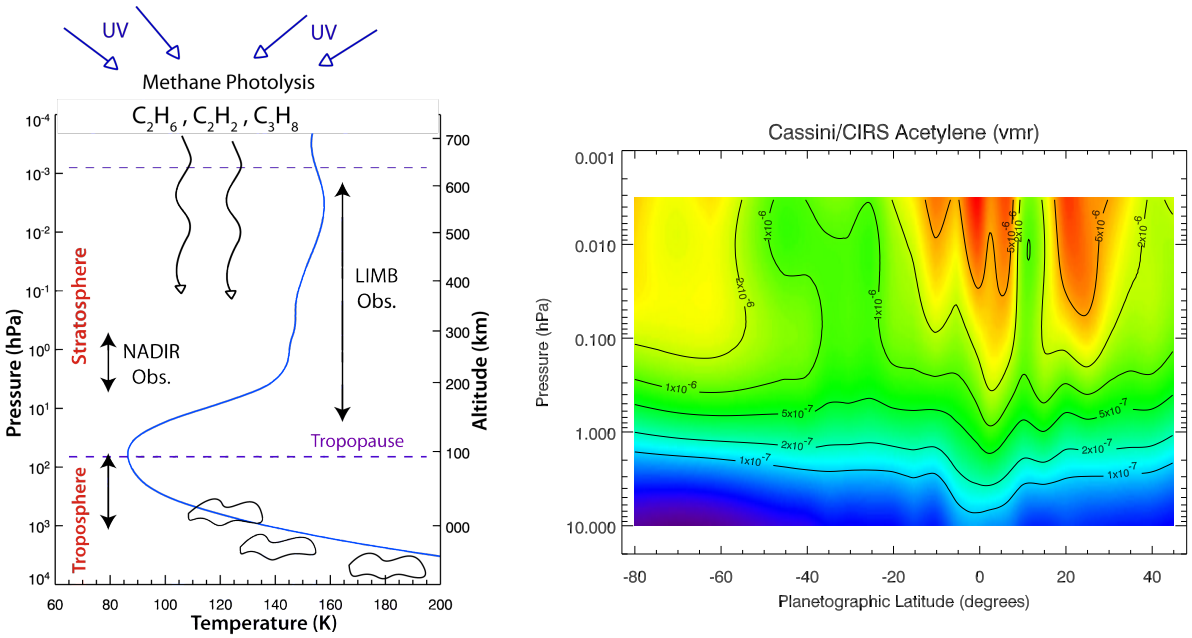

Fig. 1. Left: Example of a Saturn's atmospheric temperature profile with altitude and pressure, along with the vertical sensitivity of limb and nadir spectroscopic observations. **Right:** Map of the volume mixing ratio of acetylene (C_2H_2) with latitude and pressure, from 2005 and 2006 Cassini/CIRS limb data analysis.

2 Results from Cassini/CIRS data analysis

2.1 Anomalies observed in trace species distributions

The distribution of several hydrocarbons based on Cassini/CIRS measurements has been discussed in details in Howett et al. (2007); Hesman et al. (2009); Sinclair et al. (2013) from nadir data analysis and in Guerlet et al. (2009, 2010) from limb data analysis. An example of the distribution of C_2H_2 based on limb observations is presented in Fig. 1 . The most striking feature is that in the lower stratosphere (below the 1 mbar pressure level), acetylene's meridional distribution is symmetric with respect to the equator (C_2H_2 decreases towards both poles), while in the upper stratosphere its meridional distribution is strongly asymmetric, with about 5 times more C_2H_2 at 30N than at 30S (Guerlet et al. 2009). A similar asymmetry at high altitudes is found for C_2H_6. However, in the lower stratosphere, its distribution differs from that of C_2H_2, as we find that C_2H_6 concentration does not vary significantly with latitude (Guerlet et al. 2009). Other studies based on CIRS nadir data and ground-based data, which probe the lower stratosphere, revealed a similar behaviour at the 2-mbar pressure level. We also note that on Jupiter, a similar configuration of the C_2H_6 and C_2H_2 distribution at 2-mbar was determined from Cassini/CIRS data analysis (Nixon et al. 2007), as the spacecraft flew by Jupiter in 2000.

Seasonal photochemical models developed for Satun's atmosphere (Moses & Greathouse 2005) predict that ethane and acetylene should have long photochemical lifetimes in the lower stratosphere (about 700 and 100 years at 2 mbar, respectively), much longer than Saturn's year (30 Earth years). Consequently, their distribution should follow the yearly averaged solar insolation, ie be maximum at the equator and decrease towards both poles. Acetylene was found to follow this trend, whereas ethane was found to either slightly increase towards the south pole, or remain constant with latitude (depending on the studies). This was interpreted as the consequence of a global meridional distribution by dynamics from the equator to the poles, which would efficiently transport the long-lived C_2H_6 but much less efficiently C_2H_2, that is more rapidly destructed by photodissociation than transported. This provided an estimation of the timescale of this global circulation, in between the two photochemical lifetimes of the considered species, i.e. 100 to 700 years.

First attempts to reproduce the observed distribution of hydrocarbons in the lower stratosphere of Saturn and Jupiter using simple dynamical assumptions have failed. Indeed, two models coupling photochemistry and eddy mixing have been tested (Liang et al. (2005) for Jupiter and Moses et al. (2007) for Saturn) but none could simultaneously reproduce the C_2H_2 and C_2H_6 distribution with realistic values of eddy mixing coefficients. One

difficulty lies in the chemical coupling between C_2H_6 and C_2H_2: when ethane is transported towards the poles, its photodissociation should also lead to producing more C_2H_2, in a way such that the two molecules should exhibit rather uniform distributions. A full General Circulation Model is thus needed to investigate transport by circulation cells (and not only by eddy mixing), to try to reproduce the observations and to investigate whether the current difference between the models and the reality arises from a dynamical or chemical origin.

At higher altitudes (at the 0.01 mbar level), hydrocarbons' lifetimes are shorter and these species are now influenced by seasonal variations of solar irradiation. The photochemical model of Moses & Greathouse (2005) predict that at the subsolar point (at about 30S at this time), photochemical production is maximum, thus hydrocarbon abundance should be high. On the other hand, under the shadow of the rings (at 25N at this time) photochemical production is low, thus the abundance should show a dip at these latitudes. Limb observations revealed the exact opposite pattern, with a sharp, local maximum of hydrocarbons centered at 25N and a large minimum in the region 20-40S (Guerlet et al. 2009). This can be interpreted as the signature of a (seasonal) circulation cell similar to the Earth Hadley cells, or to Brewer-Dobson circulation, inducing downwelling under the ring's shadows which brings hydrocarbon-rich air. This is the first evidence of a seasonal circulation pattern on a giant planet.

Finally, limb data acquired by Cassini/CIRS also have the advantage to increase the sensitivity to trace species (as the lightpath is increased). Using this technique, maps of propane, methylacetylene and diacetylene have been obtained for the first time in the lower stratosphere (Guerlet et al. 2010). Having different lifetimes than ethane and acetylene, these minor species can potentially be employed as dynamical tracers and improve the constraints on atmospheric dynamics, although a full dynamical model is needed to exploit this information and yield more quantitative constraints on the circulation.

2.2 Anomalies in the temperature field

Cassini/CIRS data analysis also provided detailed maps of the stratospheric temperature. From the resolution of the thermal wind equation, zonal wind maps could also be derived. Those maps led to the discovery of Saturn's equatorial oscillation (Fouchet et al. 2008), characterized by alternate bands of eastward and westward jets with altitude at the equator, and alternate extrema of temperature. Its period has been estimated to half a kronian year from ground-based observations (Orton et al. 2008) and from the study of the descending pattern with time (Guerlet et al. 2011). A similar oscillation have been discovered in Jupiter's stratosphere (Friedson, 1999, Simon-Miller et al., 2007). Both are qualitatively analogous to the Earth's QBO (Quasi-Biennal Oscillation), a dynamical phenomenon triggered by the interaction between waves and the mean zonal flow. This represents a good example of comparative planetology, and these multiple observations are a unique opportunity to learn more about equatorial oscillations in general. These oscillations have different periods on the three planets and the wave activity is supposedly quite different, although weakly characterized for Jupiter and Saturn.

Modeling of the Quasi-Quadriennal Oscillation on Jupiter (QQO) indicated that most of the previously observed planetary-scale Rossby waves were not a likely cause for the Jupiter QQO, but could not be ruled out as a contributing factor. Other waves, depositing energy in the upper troposphere ($\sim$300 mbar), were able to somewhat reproduce a QQO signal in the stratosphere (Friedson 1999; Li & Read 2000), but predicted a much larger QQO amplitude in actual temperature than was found in earlier brightness temperature analyses. Numerical efforts, coupled to more observations and characterization of waves, are thus still needed to try to reproduce the equatorial oscillations and understand their different periods.

The meridional temperature profiles also exhibit features left unexplained by the predictions of a seasonal radiative transfer model (that of Greathouse et al. (2008) applied by Fletcher et al. (2010)). The model predicts that under the ring's shadow the temperature should significantly decrease, by 10 to 20K with respect to the surrounding latitudes. This effect should be visible in the whole stratosphere (20 mbar to 10^{-2} mbar). However, this low temperature region is not visible in Cassini/CIRS observations. We interpret this as another sign of the seasonal circulation cell that we mentioned earlier. Indeed, downwelling below the ring's shadow will not only enrich the atmosphere in hydrocarbons, it would also likely warm up the stratosphere by adiabatic compression. As the radiative equilibrium model of Greathouse et al. (2008) did not include dynamics, this assumption could not be tested and quantified.

3 Conclusions

Cassini/CIRS nadir and limb data analysis have allowed to map Saturn's stratospheric thermal structure and the distribution of hydrocarbons, by-products of a complex photochemistry. These results have revealed anomalies that cannot be explained by current seasonal radiative or photochemical models. Another example of anomaly not discussed here is the spectacularly warm anticyclone that developed in the stratosphere after the December 2010 Great White Storm (Fletcher et al. 2012). All these features hint at complex atmospheric dynamical phenomena at play and advocate for the development of a General Circulation Model (GCM) of Saturn's upper troposphere and stratosphere. Such a GCM is currently under development at the Laboratoire de Meteorologie Dynamique, where we benefit from the experienced gained through the development of GCMs for the atmospheres of the Earth, Mars, Venus, Titan and even exoplanets (Forget et al. 1999; Wordsworth et al. 2011).

We also emphasize that future observations (by Cassini's extended mission till 2017, as well as ground-based) remain crucial to bring more constraints on our understanding of how giant planets' atmosphere behave and evolve.

We acknowledge funding from the French ANR under grant agreement ANR-12-PDOC-0013.

References

Fletcher, L. N., Achterberg, R. K., Greathouse, T. K., et al. 2010, Icarus, 208, 337
Fletcher, L. N., Hesman, B. E., Achterberg, R. K., et al. 2012, Icarus, 221, 560
Forget, F., Hourdin, F., Fournier, R., et al. 1999, J. Geophys. Res., 104, 24155
Fouchet, T., Guerlet, S., Strobel, D. F., et al. 2008, Nature, 453, 200
Friedson, A. J. 1999, Icarus, 137, 34
Greathouse, T. K., Strong, S., Moses, J., et al. 2008, in AGU Fall Meeting Abstracts, B6+
Guerlet, S., Fouchet, T., Bézard, B., Flasar, F. M., & Simon-Miller, A. A. 2011, Geophys. Res. Lett., 38, 9201
Guerlet, S., Fouchet, T., Bézard, B., et al. 2010, Icarus, 203, 214
Guerlet, S., Fouchet, T., Bézard, B., Simon-Miller, A. A., & Flasar, F. 2009, Icarus, 203, 214
Hesman, B. E., Jennings, D. E., Sada, P. V., et al. 2009, Icarus, 202, 249
Howett, C. J. A., Irwin, P. G. J., Teanby, N. A., et al. 2007, Icarus, 190, 556
Li, X. & Read, P. L. 2000, Planet. Space Sci., 48, 637
Liang, M.-C., Shia, R.-L., Lee, A. Y.-T., et al. 2005, ApJ, 635, L177
Moses, J. I. & Greathouse, T. K. 2005, Journal of Geophysical Research (Planets), 110, 9007
Moses, J. I., Liang, M.-C., Yung, Y. L., & Shia, R.-L. 2007, in Planetary Atmospheres, 85–86
Nixon, C. A., Achterberg, R. K., Conrath, B. J., et al. 2007, Icarus, 188, 47
Orton, G. S., Yanamandra-Fisher, P. A., Fisher, B. M., et al. 2008, Nature, 453, 196
Sinclair, J. A., Irwin, P. G. J., Fletcher, L. N., et al. 2013, Icarus, 225, 257
Wordsworth, R. D., Forget, F., Selsis, F., et al. 2011, ApJ, 733, L48